



Article

The Antimicrobial Photoinactivation Effect on *Escherichia coli* through the Action of Inverted Cationic Porphyrin–Cyclodextrin Conjugates

Cláudia P. S. Ribeiro ¹, Maria A. F. Faustino ¹, Adelaide Almeida ^{2,*} and Leandro M. O. Lourenço ^{1,*}

¹ LAQV–REQUIMTE and Department of Chemistry, University of Aveiro, 3810-193 Aveiro, Portugal; claudia.santos.ribeiro7@ua.pt (C.P.S.R.); faustino@ua.pt (M.A.F.F.)

² CESAM and Department of Biology, University of Aveiro, 3810-193 Aveiro, Portugal

* Correspondence: aalmeida@ua.pt (A.A.); leandrolourenco@ua.pt (L.M.O.L.)

Abstract: Photodynamic action has been used for diverse biomedical applications, such as treating a broad range of bacterial infections. Based on the combination of light, dioxygen, and photosensitizer (PS), the photodynamic inactivation (PDI) approach led to the formation of reactive oxygen species (ROS) and represented a non-invasive, non-toxic, repeatable procedure for pathogen photoinactivation. To this end, different tetrapyrrolic macrocycles, such as porphyrin (Por) dyes, have been used as PSs for PDI against microorganisms, mainly bacteria. Still, there is significant room for improvement, especially new PS molecules. Herein, unsymmetrical new pyridinone (3–5) and thiopyridyl Pors (7) were prepared with α -, β -, or γ -cyclodextrin (CD) units, following their quaternization to perform the corresponding free-base Pors (3a–5a and 7a), and were compared with the already-known Pors 6a and 8a, both bearing thiopyridinium and CD units. These water-soluble porphyrins were evaluated as PSs, and their photophysical and photochemical properties and photodynamic effects on *E. coli* were assessed. The presence of one CD unit and three positive charges on the Por structure (3a–5a and 7a) enhanced their aqueous solubility. The photoactivity of the cationic Pors 3a–5a and 6a–8a ensured their potential against the Gram-negative bacterium *E. coli*. Within each series of methoxy pyridinium vs thiopyridinium dyes, the best PDI efficiency was achieved for 5a with a bacterial viability reduction of 3.5 log₁₀ (50 mW cm⁻², 60 min of light irradiation) and for 8a with a total bacterial viability reduction (>8 log₁₀, 25 mW cm⁻², 30 min of light irradiation). Here, the presence of the methoxy pyridinium units is less effective against *E. coli* when compared with the thiopyridinium moieties. This study allows for the conclusion that the peripheral charge position, quaternized substituent type/CD unit, and affinity to the outer bacterial structures play an important role in the photoinactivation efficiency of *E. coli*, evidencing that these features should be further addressed in the pursuit for optimised PS for the antimicrobial PDI of pathogenic microorganisms.

Keywords: porphyrin; methoxy pyridinium; thiopyridinium; Gram-negative bacterium; *E. coli*; planktonic form; cyclodextrins; positive charge



Citation: Ribeiro, C.P.S.; Faustino, M.A.F.; Almeida, A.; Lourenço, L.M.O. The Antimicrobial Photoinactivation Effect on *Escherichia coli* through the Action of Inverted Cationic Porphyrin–Cyclodextrin Conjugates. *Microorganisms* **2022**, *10*, 718. <https://doi.org/10.3390/microorganisms10040718>

Academic Editor: Gabriela Jorge Da Silva

Received: 28 February 2022

Accepted: 24 March 2022

Published: 26 March 2022

Publisher's Note: MDPI stays neutral with regard to jurisdictional claims in published maps and institutional affiliations.



Copyright: © 2022 by the authors. Licensee MDPI, Basel, Switzerland. This article is an open access article distributed under the terms and conditions of the Creative Commons Attribution (CC BY) license (<https://creativecommons.org/licenses/by/4.0/>).

1. Introduction

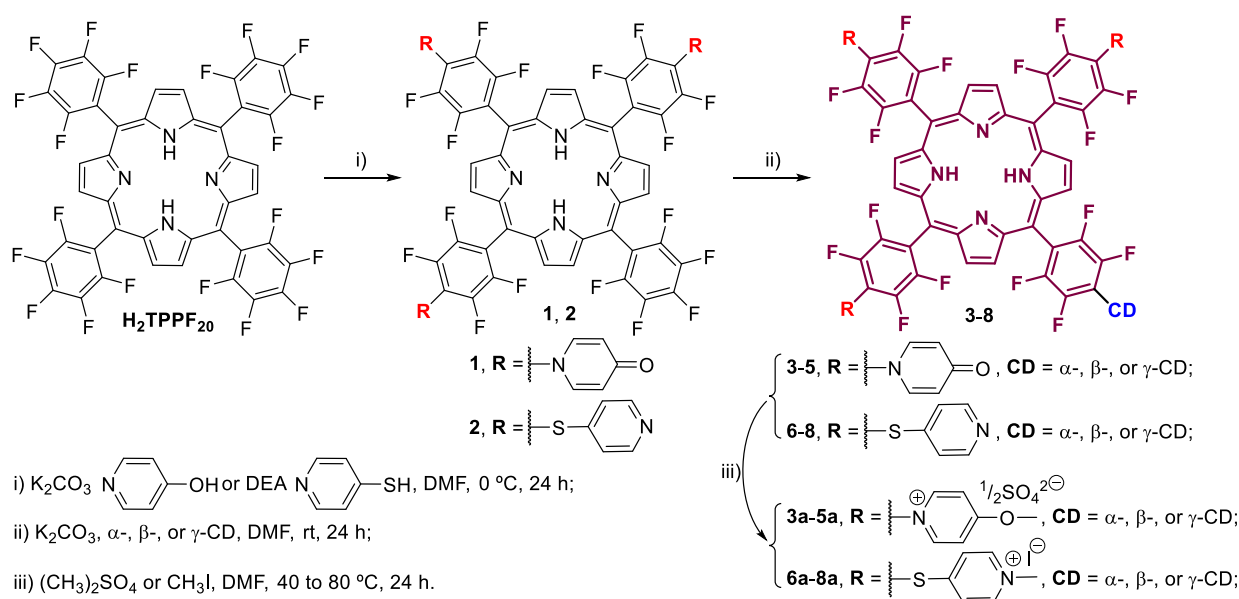
Escherichia coli belongs to the *Enterobacteriaceae* family, considered pathogenic Gram-negative bacteria. This bacterium is present in the intestinal microbiome of humans [1]. However, some strains can promote disease. Many of them cause severe infections in the urinary tract, digestive system, or even in the blood [2]. In recent decades, an increase in microbial resistance against antibiotics has been witnessed. *E. coli* is no exception and, thus, it is essential to find an alternative for its effective combat [3].

One of the interesting alternatives that have been studied, with promising results, is the antimicrobial photoinactivation (PDI) approach. PDI is based on the use of three key elements: the photosensitizer (PS), light source, and dioxygen (O₂), which, when combined, promote the production of reactive oxygen species (ROS) and free radicals,

inducing oxidative damage in biological targets [4,5]. This method can be applied in different microorganisms, such as bacteria [6], viruses [7], fungi [8], and protozoa [9]. Thus, the PDI approach has been explored for, e.g., surface disinfection [10], wastewater treatment [11], or food decontamination [12,13].

The selection of the PS is essential, which must be fast, efficient, and selective. Numerous molecules can be considered PSs, such as chlorin (Chl) [4,14–16], porphyrin (Por) [6,17–19], and phthalocyanine (Pc) dyes [5,20–26]. The PDI's effectiveness is also influenced by the microorganism structure. The cell wall complexity of Gram-negative bacteria is higher than that of Gram-positive ones. However, their porous cell wall allows the crossing and accumulation of PS [21,27,28]. To improve the PS biodistribution, finding suitable PS chemical structures and solubility strategies are necessary. Some published studies demonstrated that cationic PSs have a higher efficacy against Gram-negative bacteria than neutral or anionic compounds [29,30]. The addition of positive charges on the Por periphery can also increase its photophysical properties and may result in an effective increase in the PDI treatment [31,32]. Moreover, binding porphyrin derivatives to amphiphilic molecules may be another strategy to adopt to increase their compatibility and biological efficacy [33–35]. Thus, the association between unsymmetrical porphyrins and versatile cyclodextrin (CD) units is extremely important for promoting water-soluble PS drugs [17]. This association with cyclic oligosaccharides derivatives, such as α -, β -, or γ -cyclodextrin (α -, β -, or γ -CD) units have been explored in drug design due to their water solubility, low toxicity, and low inflammatory response [36–38]. Moreover, CDs present several strategies for combating microbial infections, including reducing resistance to known antibiotics by altering the possibility of cell-to-cell communication (quorum sensing), thus reducing the likelihood of resistance [39–41]. Given these properties and those of porphyrins, it was decided to bring both together and try to increase the PDI efficacy against bacteria.

Here, we synthesized water-soluble porphyrin–cyclodextrin (Por–CD) conjugates to assess their photodynamic efficiency against *E. coli*, a Gram-negative bacterial model. We compared the effectiveness of Por–CD conjugates (with three positive charges) bearing methoxypyridinium (3a–5a) and thiopyridinium (6a–8a) moieties to photoinactivate the *E. coli*. The new synthesized unsymmetrical Pors 3a–5a and 7a, covalently linked to the α -, β -, or γ -CD units, were compared with the already-known Pors 6a and 8a (Scheme 1).



Scheme 1. Cationic porphyrin-cyclodextrin conjugates.

2. Experimental Procedure

2.1. General

All reagents were acquired from Sigma-Aldrich (St. Louis, MO, USA) with high purities and were immediately used in the reactions. In some cases, standard procedures were applied on the solvents, such as distillation or drying [42]. Thin-layer chromatography (TLC) was performed in silica (Merck 60, 0.2 mm thick). Chromatography of the column was made in silica (Merck, Kenilworth, NJ, USA, 35–70 mesh). ^1H (300.13 MHz) and ^{19}F (282.38 MHz) NMR spectra were acquired in Bruker Avance-300 spectrometers. It was used as an internal reference of tetramethylsilane (TMS) and the deuterium solvent of dimethyl sulfoxide ($\text{DMSO-}d_6$). Chemical shifts were determined in δ (ppm), and coupling constants (J) in Hertz (Hz). ESI-MS spectra were acquired on an instrument of Q-TOF 2 (Micromass, Manchester, UK). Sample solutions were prepared at 1 mg/mL in MeOH or H_2O . The absorbance and steady-state fluorescence spectra of Pors (**3a–8a**) were recorded in dimethyl sulfoxide (DMSO) in quartz optical cells at 298 K and under normal air conditions by using Shimadzu UV-2501PC and the spectrofluorometer FluoroMax Plus, Horiba, respectively. The fluorescence quantum yield (Φ_{F}) of the Pors was calculated by comparing the area under the emission spectrum of every compound, with the area under the emission spectrum of 5,10,15,20-tetraphenylporphyrin (TPP) ($\Phi_{\text{F}} = 0.13$ in DMSO) as a standard reference [43].

2.2. Synthesis of 5-(pentafluorophenyl)-10,15,20-tris[2,3,5,6-tetrafluoro-4-(4-oxopyridin-1(4H)-yl)phenyl]porphyrin, Por 1

In a 50 mL round-bottom flask, 5,10,15,20-tetrakis(pentafluorophenyl)porphyrin ($\text{H}_2\text{TPPF}_{20}$, 300.3 mg, 3.1×10^{-4} mol, 1 eq.) and 4-hydroxypyridine (90.8 mg, 9.5×10^{-4} mol, 3.1 eq.) were dissolved in 10 mL of DMF under an N_2 atmosphere. After stirring during the 48 h at r.t., the TLC analysis confirmed that the nucleophilic reaction was complete. The DMF was completely evaporated under reduced pressure. The crude reaction was dissolved in a mixture of $\text{CH}_2\text{Cl}_2/\text{MeOH}$ (93/7, v/v%) and purified by column chromatography using the same eluent. The main fraction was subsequently precipitated in hexane, filtrated, and washed with the same solvent. The obtained purple solid was dried under a vacuum system over 6 h at 80 °C. Yield (Por 1): 80% (297.6 mg, 3.3×10^{-4} mol).

^1H NMR (300.13 MHz, $\text{DMSO-}d_6$): δ -3.14 (s, 2H, -NH), 6.55 (d, $J = 7.7$ Hz, 6H, *m*-H), 8.23 (d, $J = 7.7$ Hz, 6H, *o*-H), 9.45–9.50 (m, 8H, β -H) ppm. ^{19}F NMR (282.38 MHz, $\text{DMSO-}d_6$): δ -158.67–-158.48 (m, 2F, Ar-F), -149.75 (t, $J = 22.6$ Hz, 1F, Ar-F), -145.42–-145.21 (m, 6F, Ar-F), -135.32 (dd, $J = 26.0, 7.6$ Hz, 2F, Ar-F), -135.07 –-134.88 (m, 6F, Ar-F) ppm. ESI-MS m/z : 1200.4 $[\text{M}+\text{H}]^+$ and 601.0 $[\text{M}+2\text{H}]^{2+}$.

2.3. Synthesis of Por-CD Conjugates, Pors 3–5

In a 25 mL round-bottom flask, a mixture of Por 1 (100 mg, 8.3×10^{-5} mol) and α -(105 mg, 1.1×10^{-4} mol), β -(123 mg, 1.1×10^{-4} mol), or γ -cyclodextrin (140 mg, 1.1×10^{-4} mol) was dissolved in 5 mL of DMF. The reaction was carried out for 72 h at 60 °C under an N_2 atmosphere, allowing for the nucleophilic substitution, also confirmed by TLC. The solvent was removed under reduced pressure and the reactional crude was dissolved in MeOH, then precipitated with water, filtered, and washed with cool water. The obtained purple solids were dried under a vacuum system over 6 h at 80 °C. The desired porphyrin-cyclodextrin conjugates were obtained in moderate yields (Por 3: 47%, Por 4: 58%, and Por 5: 41%).

5-[4-(α -cyclodextrin)-2,3,5,6-tetrafluoro]-10,15,20-tris[2,3,5,6-tetrafluoro-4-(4-oxopyridin-1(4H)-yl)phenyl]porphyrin, Por 3: ^1H NMR (300.13 MHz, $\text{DMSO-}d_6$): δ -3.08 (br s, 2H, -NH), 6.28–6.54 (m, 6H, *m*-H), 7.96–8.30 (m, 6H, *o*-H), 9.14–9.65 (m, 8H, β -H) ppm. ^{19}F NMR (282.38 MHz, $\text{DMSO-}d_6$): δ -145.98–-144.86 (m, 8F, Ar-F), -135.00–-133.69 (m, 8F, Ar-F) ppm. ESI-MS m/z : 1076.3 $[\text{M}+2\text{H}]^{2+}$ and 710.9 $[\text{M}+3\text{H}]^{3+}$. UV-Vis (DMSO): λ (log ϵ) 417 (4.17); 510 (2.01); 583 (1.47) nm.

5-[4-(β -cyclodextrin)-2,3,5,6-tetrafluoro]-10,15,20-tris[2,3,5,6-tetrafluoro-4-(4-oxopyridin-1(4*H*)-yl)phenyl]porphyrin, Por 4: ^1H NMR (300.13 MHz, $\text{DMSO-}d_6$): δ -3.03 (br s, 2H, -NH), 6.27–6.76 (m, 6H, *m*-H), 7.92–8.20 (m, 6H, *o*-H), 9.22–9.43 (m, 8H, β -H) ppm. ^{19}F NMR (282.38 MHz, $\text{DMSO-}d_6$): δ -146.31–145.17 (m, 8F, Ar-F), -135.57–134.55 (m, 8F, Ar-F) ppm. ESI-MS *m/z*: 1157.5 [$\text{M}+2\text{H}$] $^{2+}$ and 773.3 [$\text{M}+3\text{H}$] $^{3+}$. UV-Vis (DMSO): λ (log ϵ) 417 (3.59); 509 (2.14); 584 (1.83) nm.

5-[4-(γ -cyclodextrin)-2,3,5,6-tetrafluoro]-10,15,20-tris[2,3,5,6-tetrafluoro-4-(4-oxopyridin-1(4*H*)-yl)phenyl]porphyrin, Por 5: ^1H NMR (300.13 MHz, $\text{DMSO-}d_6$): δ -3.09 (br s, 2H, -NH), 6.39–6.66 (m, 6H, *m*-H), 7.83–8.40 (m, 6H, *o*-H), 9.17–9.75 (m, 8H, β -H) ppm. ^{19}F NMR (282.38 MHz, $\text{DMSO-}d_6$): δ -146.92–144.68 (m, 8F, Ar-F), -135.72–133.87 (m, 8F, Ar-F) ppm. ESI-MS *m/z*: 1239.5 [$\text{M}+2\text{H}$] $^{2+}$ and 827.0 [$\text{M}+3\text{H}$] $^{3+}$. UV-Vis (DMSO): λ (log ϵ) 418 (3.96); 510 (2.03); 584 (1.56) nm.

2.4. Synthesis of Cationic Por-CD Conjugates, Pors 3a–5a

In a sealed tube, Por 3 (50 mg, 2.3×10^{-5} mol), Por 4 (50 mg, 2.2×10^{-5} mol), or Por 5 (50 mg, 2.0×10^{-5} mol) was dissolved in 5 mL of DMF and reacted with an excess of $(\text{CH}_3)_2\text{SO}_4$ (3.0 mL). The reaction was stirred overnight at 80 °C. After this period, the reaction tube was cooled to room temperature and the reactional mixture was precipitated with CH_2Cl_2 (6 mL), filtered, and washed with the same solvent. The obtained purple solids were dried under a vacuum system over 6 h at 80 °C and the cationic derivatives were obtained in moderate-to-good yields (Por 3a (35 mg, 1.6×10^{-5} mol, 43%), Por 4a (38 mg, 1.6×10^{-5} mol, 73%), Por 5a (35 mg, 1.4×10^{-5} mol, 70%).

5-[4-(α -cyclodextrin)-2,3,5,6-tetrafluorophenyl]-10,15,20-tris[2,3,5,6-tetrafluoro-4-(4-methoxypyridinium-1-yl)phenyl]porphyrin, Por 3a: ^1H NMR (300.13 MHz, $\text{DMSO-}d_6$): δ -3.08 (br s, 2H, -NH), 4.37 (s, 9H, -OCH₃), 8.14–8.20 (m, 6H, *m*-H), 9.37–9.55 (m, 14H, 6 *o*-H and 8 β -H) ppm. ^{19}F NMR (282.38 MHz, $\text{DMSO-}d_6$): δ -144.35–143.47 (m, 8F, Ar-F), -133.88–133.23 (m, 8F, Ar-F) ppm. UV-Vis (DMSO): λ (log ϵ) 416 (4.04); 509 (1.84); 583 (1.35) nm.

5-[4-(β -cyclodextrin)-2,3,5,6-tetrafluorophenyl]-10,15,20-tris[2,3,5,6-tetrafluoro-4-(4-methoxypyridinium-1-yl)phenyl]porphyrin, Por 4a: ^1H NMR (300.13 MHz, $\text{DMSO-}d_6$): δ -3.08 (br s, 2H, -NH), 4.36 (s, 9H, -OCH₃), 8.06–8.20 (m, 6H, *m*-H), 9.41–9.48 (m, 14H, 6 *o*-H and 8 β -H) ppm. ^{19}F NMR (282.38 MHz, $\text{DMSO-}d_6$): δ -144.32–143.38 (m, 8F, Ar-F), -133.95–133.42 (m, 8F, Ar-F) ppm. UV-Vis (DMSO): λ (log ϵ) 417 (3.37); 509 (2.14); 583 (1.61) nm.

5-[4-(γ -cyclodextrin)-2,3,5,6-tetrafluorophenyl]-10,15,20-tris[2,3,5,6-tetrafluoro-4-(4-methoxypyridinium-1-yl)phenyl]porphyrin, Por 5a: ^1H NMR (300.13 MHz, $\text{DMSO-}d_6$): δ -3.10 (br s, 2H, -NH), 4.37 (s, 9H, -OCH₃), 8.18–8.22 (m, 6H, *m*-H), 9.34–9.53 (m, 14H, *o*-H and β -H) ppm. ^{19}F NMR (282.38 MHz, $\text{DMSO-}d_6$): δ -144.08–143.48 (m, 8F, Ar-F), -133.83–133.27 (m, 8F, Ar-F) ppm. UV-Vis (DMSO): λ (log ϵ) 417 (3.10); 510 (1.82); 583 (1.43) nm.

2.5. Synthesis of Por-CD Conjugate, Por 7

Por 2 [17] (100 mg, 8.1×10^{-5} mol) and 10 equivalents of β -cyclodextrin were dissolved in 5 mL of DMF and the reaction was stirred under an N_2 atmosphere and over 72 h at 60 °C until the confirmation, by TLC, that Por 2 was totally consumed. After the workup, the reactional residue was dissolved in MeOH and precipitated in water, filtered, and washed with water. The obtained purple solid constituted by Por 7 was dried under a vacuum system over 6 h at 80 °C. Compound 7 was obtained in a moderate yield (99 mg, 4.2×10^{-5} mol, 52%).

5-[4-(β -cyclodextrin)-2,3,5,6-tetrafluorophenyl]-10,15,20-tris[2,3,5,6-tetrafluoro-4-(pyridin-4-ylthio)phenyl]porphyrin, Por 7: ^1H NMR (300.13 MHz, $\text{DMSO-}d_6$): δ -3.08 (br s, 2H, -NH), 7.39–7.96 (m, 6H, *m*-H), 8.40–8.63 (m, 6H, *o*-H), 9.37–9.60 (m, 8H, β -H) ppm. ^{19}F NMR (282.38 MHz, $\text{DMSO-}d_6$): δ -133.65 (dd, $J = 26.4, 11.2$ Hz, 8F, Ar-F),

−128.70 (dd, $J = 26.4, 11.2$ Hz, 8F, Ar-F) ppm. ESI-MS m/z : 1187.2 $[M+2H]^{2+}$. UV-Vis (DMSO): λ (log ϵ) 420 (3.13); 510 (2.00); 588 (1.65) nm.

2.6. Synthesis of Cationic Por-CD Conjugate, Por 7a

In a sealed tube, Por 7 (50.1 mg, 2.1×10^{-5} mol) was dissolved in DMF (3.0 mL) and was added to an excess of methyl iodide (1.0 mL, 16.1 mmol). The reaction was stirred overnight at 40 °C. After this period, the reactional mixture was cooled until room temperature and the positive charged product was precipitated in CH_2Cl_2 , filtered, and washed with the same solvent. The obtained purple solid was dried under a vacuum system over 6 h at 80 °C and was recovered in excellent yield, obtaining the compound 7a (48 mg, 1.9×10^{-5} mol, 95%).

5-[4-(β -cyclodextrin)-2,3,5,6-tetrafluorophenyl]-10,15,20-tris[2,3,5,6-tetrafluoro-4-(1-methylpyridinium-4-yl-thio)phenyl]porphyrin triiodide, Por 7a: 1H NMR (300.13 MHz, DMSO- d_6): δ −3.08 (br s, 2H, -NH), 4.35 (s, 9H, N- CH_3), 8.44–8.48 (m, 6H, m -H), 8.90–9.00 (m, 6H, o -H), 9.59–9.71 (m, 8H, β -H) ppm. ^{19}F NMR (282.38 MHz, DMSO- d_6): δ −132.89–−132.76 (m, 8F, Ar-F), −128.00–−127.87 (m, 8F, Ar-F) ppm. UV-Vis (DMSO): λ (log ϵ) 420 (3.09); 514 (1.95); 588 (1.62) nm.

2.7. Photostability Assays

The PBS solutions of Pors 3a–8a (3 mL in quartz cuvettes) were irradiated under the same light conditions applied in the biological experiments. The UV-Vis spectrum was monitored, and the Soret band absorbance value (between 416 and 420 nm) of each PS (3a–8a) was displayed before (time $t_0 = Abs_0$) and after white light exposure for pre-defined intervals (5, 10, 15, 20, 25, 30, 45, and 60 min) (Abs_t):

$$Photostability (\%) = \left(\frac{Abs_t}{Abs_0} \right) \times 100$$

Light Conditions

A white light LED system (ELMARK-VEGA20, 20 W, 1400 lm, range of 400–700 nm) was used for the irradiation of the Por dyes at different irradiation intensities of 25 and 50 $mW\ cm^{-2}$. The light irradiance was determined through a Power Meter Coherent FieldMaxII196 Top with a Coherent PowerSens PS19Q energy sensor.

2.8. Singlet Oxygen Generation

Different solutions of each PS (Abs at 420 nm ≈ 0.2) were prepared in DMF with 9,10-dimethylanthracene (9,10-DMA) at a concentration of 50 μM . These solutions were irradiated in quartz cuvettes with blue light ($\lambda = 420$ nm). A solution of TPP in DMF was used as a reference ($\Phi_\Delta = 0.65$) [44,45]. The photooxidation kinetics of 9,10-DMA was studied by decaying the absorption of 9,10-DMA absorbance at 378 nm, the photooxidation results of 9,10-DMA were photosensitized by PSs 3a–8a, and the reference was registered in a first-order plot [46–48]. Three independent experiments were performed.

2.9. Bacterial Strain and Growth Conditions

The genetically transformed bioluminescent *E. coli* Top10 (by the luxCDABE genes of the marine bioluminescent bacterium *Allivibrio fischeri*) was grown in a Tryptic Soy Broth medium (TSA, Merck), enriched with 50 $mg\ mL^{-1}$ of ampicillin (Amp) and 34 $mg\ mL^{-1}$ of chloramphenicol (Cm). Before the assay, one colony was placed into a flask with Tryptic Soy Broth (TSB, Merck), enriched with Amp and Cm, and was grown at 25 °C overnight under shaking at 120 rpm. Then, an aliquot was transferred into 10 mL of TSB under the same growth conditions until the stationary growth phase was achieved. An optical density of 600 nm (OD_{600}) of 1.6 ± 0.1 corresponded to 10^8 colony forming units per millilitre ($CFU\ mL^{-1}$). The correlation of $CFU\ mL^{-1}$ and the bioluminescence signal (in relative light units, RLUs) of the bioluminescent *E. coli* is described in the literature [49].

2.10. Photodynamic Inactivation Studies

The bacteria of *E. coli* were grown overnight in TBS. After that, it was diluted in PBS (pH = 7.49) to a final concentration of $\approx 10^7$ CFU mL⁻¹, corresponding to $\sim 10^7$ RLU. This bacterial suspension was equivalently distributed in 6-well plates and a suitable volume of each PS was added in order to accomplish the final concentration of 5.0 μ M. From our previous published binding studies [17], the best concentration to minimize the aggregation effect of the PSs was 5 μ M. The experiment had a light control (LC), which contained only the bacterial suspension, as well as a dark control (DC), which included the bacterial suspension incubated with the PS at 5.0 μ M and was protected from light. Both were exposed to the same irradiation conditions as the samples. The samples and the controls were protected from light using aluminum foil and were kept in the dark for 15 min to provide the ability of PS to bind to *E. coli*. At the end of the incubation process, all the samples were irradiated under agitation for 60 min at 20 °C. Aliquots of 1.0 mL were collected and the bacterial bioluminescence was measured in a luminometer (TD-20/20 Luminometer, Turner Designs, Inc., Madison, WI, United States). The detection limit of the equipment is ca. 2.3 log. Three independent experiments were performed.

In addition to measuring bioluminescence, aliquots of treated and control samples were taken from the first and last time points, serially diluted, and poured in triplicate onto a Tryptic Soy Agar (TSA) medium. The plates were incubated for 24 h at a controlled temperature of 37 °C, and the concentration of the viable cells was determined by counting the CFU. At least three independent experimental measurements were conducted with three replicates. The results are determined as the average of the three assays.

2.11. Statistical Analysis

At least three independent experiments, with three replicates per assay for each condition, were done. The statistical analysis was performed with GraphPadPrism 8. The Kolmogorov–Smirnov test was used to check for normal distributions, and the homogeneity of variance was verified with the Brown–Forsythe test. ANOVA and Dunnett’s multiple comparison tests were applied to assess whether the samples were statistically significant.

3. Results and Discussion

3.1. Synthesis, Photophysical, and Photochemical Characterization of the Porphyrin Derivatives

The neutral tri-substituted 4-pyridinone, Pors **1** and **3–5**, and the cationic Pors **3a–5a** (Scheme 1), were prepared through a nucleophilic substitution methodology well-established in our research group [50]. The tri-substituted 4-pyridinone Por **1** was prepared from commercial H₂TPPF₂₀ using three equivalents of 4-hydroxypyridine and K₂CO₃ in DMF as the solvent. Pors **3–5** was synthesized from Por **1** after the reaction with ~ 1.2 equivalents of the corresponding α -, β -, or γ -cyclodextrin (Scheme 1), where the reactional temperature was carefully controlled. The cationic Pors **3a–5a** was attained by a quaternization process using an excess of dimethyl sulfate in DMF at 80 °C. It is worth noting that the quaternization of the pyridinone groups from **3–5** requires higher temperatures when compared with the quaternization of pyridyl groups **6–8** which occurs at 40 °C. Although the neutral Pors **3–5** were isolated with moderate yields (47%, 58%, and 41%, respectively), the cationic derivatives **3a–5a** were achieved in good yields (43%, 73%, and 70%, respectively). The substituted Pors were synthesized following experimental procedures established in our research group [17]. Por **2** (Scheme 1) was prepared from the H₂TPPF₂₀ by the nucleophilic substitution with three equivalents of 4-mercaptopyridine in DMF. The neutral Pors **6–8** were synthesized from Por **2** with one α -, β -, or γ -cyclodextrin unit (Scheme 1) via nucleophilic substitution. The cationic Pors **6a–8a** were obtained from the cationization of Pors **6–8**, respectively, with methyl iodide in DMF. All Por structures were confirmed by ¹H and ¹⁹F NMR spectroscopy, ESI–MS spectrometry (when it was possible to determine), and were characterized by UV–Vis absorption and emission spectroscopy (Figure 1).

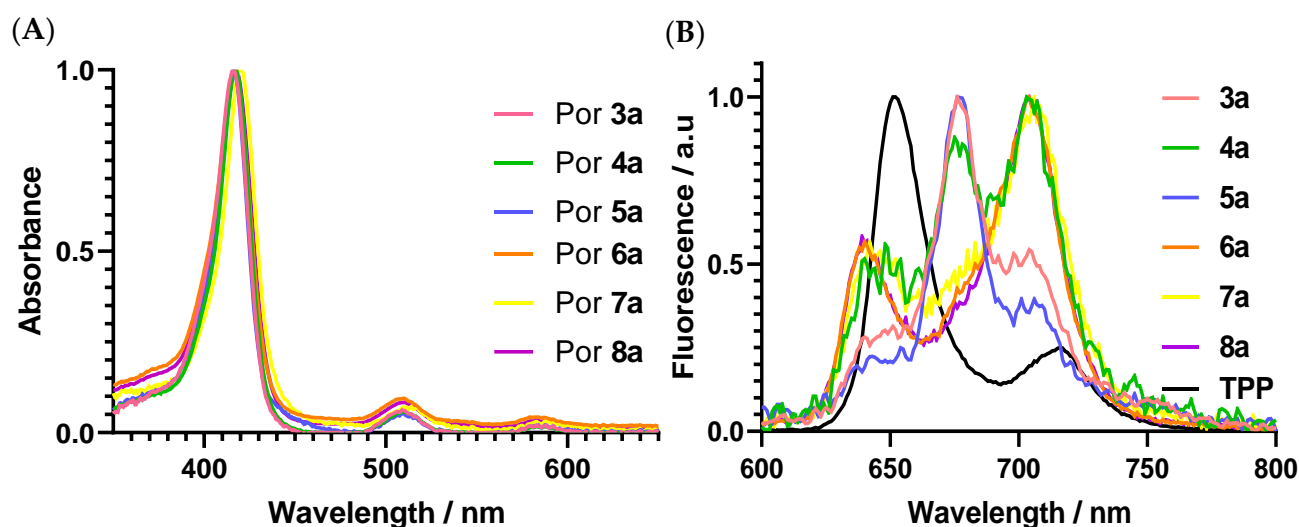


Figure 1. Normalized (A) absorption and (B) emission spectra of Pors 3a–8a in DMSO at 298 K.

The ^1H NMR spectrum of the Por 1 is characteristic of a trisubstituted pattern, evidencing two doublets at δ 6.55 ppm and δ 8.23 ppm ($J = 7.7$ Hz) corresponding to the resonance of 6 *meta*-protons and 6 *ortho*-protons on the 4-pyridinone groups, respectively. Additionally, the ^{19}F NMR spectrum of Por 1 is compatible with a *para* substitution pattern of three pentafluorophenyl rings and one unsubstituted pentafluorophenyl ring. The ^{19}F NMR spectra of Pors 3–5 revealed the disappearance of the signal at -149.75 ppm due to the *para*-fluorine replacement by the cyclodextrin and the appearance of two multiplets on the interval of $\delta -146.92$ – -144.68 ppm and $\delta -135.72$ – -133.69 ppm, corresponding these signals to the *ortho*- and *meta*-fluorine atoms. The cationization of the neutral compounds provided to the Pors 3a–5a were confirmed by the appearance of the singlet in the aliphatic region located at δ 4.36–4.37 ppm of the ^1H NMR, which corresponds to the resonance of the $-\text{OCH}_3$ protons.

The ESI–MS analysis shows the observed species resulting from the characteristic fragmentation processes of these Pors with the formation of species with different overall m/z ratios.

3.1.1. Photophysical and Photochemical Studies

The absorption spectra of cationic Pors 3a–8a were recorded in DMSO solutions ($\sim 10^{-5}$ M) at 298 K (Figure 1). The UV–Vis absorption spectra of the new Pors 3a–5a and 7a in DMSO solutions exhibit a typical feature of *meso*-substituted porphyrin derivatives with a strong Soret band at ca. 418 nm and weak Q bands between 500 and 650 nm (Figure 1). Moreover, although free-base porphyrins generally display four Q bands, *meso*-pentafluorophenylporphyrin derivatives often display only two Q bands, with the remaining two Q bands as indefinite. It is worth noting that the Soret bands of Pors 3a–5a and 7a appear slightly broadened in the base, typical of the aggregation phenomena. All the studied derivatives showed weak emissive properties with fluorescence quantum yields above 1% [6,50]. This fact might be due to a non-radiative excited deactivation that is very likely due to aggregation phenomena observed in DMSO for the tricationic dyes conjugated with a CD unit.

The absorption characteristics, molar extinction coefficients (ϵ), and fluorescence quantum yield for Pors 3a–8a in DMSO are summarized in Table 1.

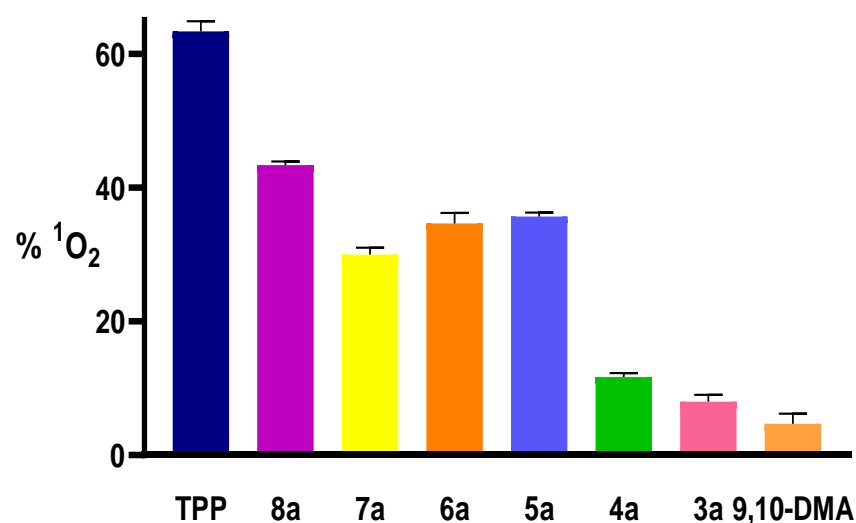
Table 1. Absorption and emissive properties of Pors **3a–8a** in DMSO.

Pors	Soret Band (nm)	log ϵ	Q Bands (nm)	log ϵ	$\lambda_{\text{emiss.}}$	Φ_F^a
3a	416	4.04	509	1.84	676	0.01
			583	1.35		
4a	417	3.37	509	2.14	704	<0.01
			583	1.61		
5a	417	3.10	510	1.82	677	<0.01
			583	1.43		
6a^b	417	3.49	510	3.43	704	<0.01
			583	3.13		
7a	420	3.09	514	1.95	706	0.01
			588	1.62		
8a^b	420	3.78	510	2.70	704	<0.01
			583	2.30		

^a Using TPP ($\Phi_F = 0.13$) as reference in DMSO [43]; ^b From reference [17].

As previously mentioned, one of the key characteristics of a molecule that is considered a PS is its ability to generate singlet oxygen ($^1\text{O}_2$), one of the main ROS responsible for causing cell damage, leading to cell death.

Thus, the production of $^1\text{O}_2$ by Pors **3a–8a** in DMF was evaluated by decaying the absorption of 9,10-DMA at 378 nm under light irradiation. No significant photodegradation of 9,10-DMA in DMF was observed without any PS under light irradiation. The generation of $^1\text{O}_2$ by the new cationic Pors (**3a–5a** and **7a**) was compared to the known cationic Pors **6a**, **8a**, and a TPP reference ($\Phi_\Delta = 0.65$ in DMF) that is considered a good generator of $^1\text{O}_2$ [44,45]. According to the obtained results summarised in Figure 2, all derivatives can generate $^1\text{O}_2$ after light exposure. The gamma-cyclodextrin Por derivatives **5a** and **8a** are the best producers of $^1\text{O}_2$ among the three cyclodextrins (α -, β -, and γ -derivatives) assessed. Comparing methoxypyridinium Por-CD dyes (**3a–5a**) with the corresponding thiopyridinium Por-CD dyes (**6a–8a**) [17], the results point out that thiopyridinium porphyrin derivatives display a higher ability to generate $^1\text{O}_2$ species.

**Figure 2.** % $^1\text{O}_2$ generation by Por-CD dyes **3a–8a** in DMF at 298 K.

Since the application purpose is the use of Por-CD derivatives **3a–8a** under light conditions to photoinactivate *E. coli*, their photostability was studied by monitoring the

absorption decay of the Soret band after irradiation with white light (400–800 nm) at an irradiance of 50 mW cm⁻² for 60 min. The obtained results are summarized in Table 2.

Table 2. Photostability of Pors **3a–8a** in PBS after 60 min of white light irradiation at an irradiance of 50 mW cm⁻².

Pors	3a	4a	5a	6a	7a	8a
% Abs decay ^a	6	8	6	14	11	9

^a Measured at Soret band wavelength.

The Por-CD conjugates **3a–8a** showed excellent photostability in PBS solution, showing a robust behavior facing the irradiation used, with 86% to 94% of the porphyrin conjugates remaining unaltered after irradiation with white light at an irradiance of 50 mW cm⁻² for 60 min (Table 2). It is worth noting that the Soret absorbance of these compounds in the dark decays ca. 3%. These absorption decreases might be related to a slight aggregation phenomenon that occurred in PBS.

3.1.2. Photodynamic Inactivation of *Escherichia coli*

The photodynamic efficiency of the cationic derivatives Por-CD was assessed against a bioluminescent *E. coli* strain Top10. The PDI efficiency of Pors **3a–5a** against the bioluminescent *E. coli* was evaluated at 5.0 μM under white light exposure at an irradiance of 25 mW cm⁻² (Figure 3A) and 50 mW cm⁻² (Figure 3B). The photodynamic efficiency of all Pors (**3a–8a**) (methoxypyridinium (**3a–5a**) and thiopyridinium (**6a–8a**)) was compared for the conditions of 5.0 μM and 25 mW cm⁻² (Figure 4). As observed in Figure 3, no bacterial decay under the light conditions occurred in the absence of PS (data provided by the light control, LC) and the presence of the PS in the absence of light (data provided by the dark control, DC). It should be noted that the *E. coli* viability was not significantly affected by the cationic inverted Pors **3a–5a** at the light exposure at an irradiance of 25 mW cm⁻² (60 min, Figure 3A). However, Por **5a** caused a slight *E. coli* photoinactivation, with a bioluminescence signal decrease of ~1.5 log₁₀ (ANOVA, *p* < 0.0001). Nevertheless, when the light irradiance used was increased twice (50 mW cm⁻², Figure 3B), the Por **5a** achieved a better PDI effect against the bioluminescent *E. coli*, with a ~3.5 log₁₀ and 4.0 log₁₀ reduction (ANOVA, *p* < 0.0001) after 30 and 60 min of light exposure, respectively, followed by Pors **4a** and **3a** (~2.5 log₁₀ and ~3.0 log₁₀, ANOVA, *p* < 0.0001) for the same light exposition time. The results point out the importance of the ¹O₂ generation by the PS. The photodynamic efficiency, to photoinactivate *E. coli*, of each PS **3a–5a** (Figure 3B) correlates with the ¹O₂ generation (Figure 2), in which the ¹O₂ production follows the ascending efficiency order (**3a** < **4a** < **5a**).

Comparing inverted methoxypyridinium Pors **3a–5a** and thiopyridinium Pors **6a–8a** at a concentration of 5.0 μM and an irradiance of 25 mW cm⁻² (Figure 4), it was observed that the *E. coli* photoinactivation occurs faster mainly in the presence of Pors **6a** and **8a**. Once again, this highlights the importance of the ¹O₂ generation by the PS, reaching the detection limit of the methodology between 30–60 min of irradiation [17]. Pors **3a–5a**, at an irradiance of 50 mW cm⁻², were less effective in the photoinactivation of the bioluminescent *E. coli* strain than the Pors **6a–8a**, even at an irradiance of 25 mW cm⁻². This fact can be explained by the positive charge localization in the thiopyridinium conjugates (**6a–8a**) in an external position. Additionally, the cationic substituent type/CD unit and affinity to the outer bacterial structures cannot be ruled out. Overall, within each series of quaternized dyes (methoxypyridinium vs. thiopyridinium), the best PSs candidates were the cationic Por-γ-CD dyes **5a** and **8a** at irradiances of 50 mW cm⁻² and 25 mW cm⁻², respectively.

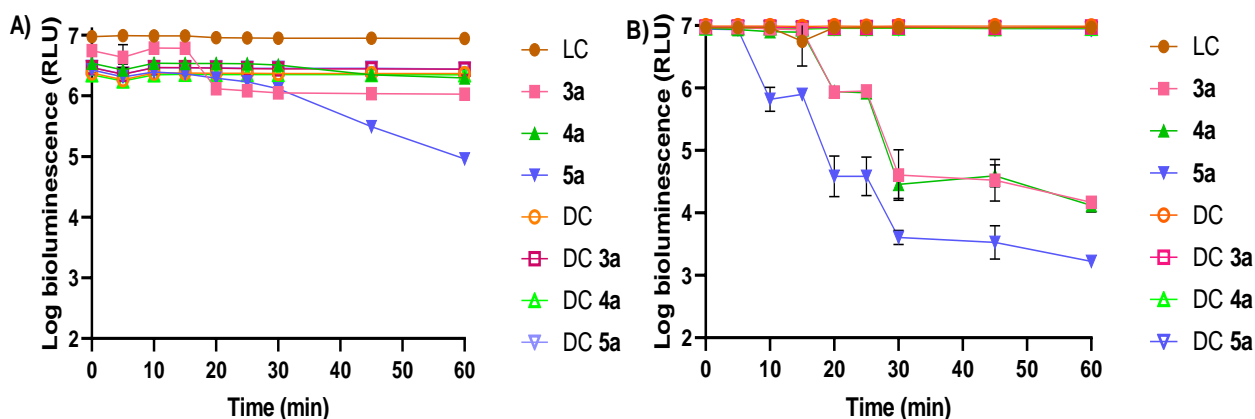


Figure 3. Bioluminescence monitoring of *E. coli* treated with PSs Por 3a–5a at 5.0 μM at different irradiation times, under white light irradiation at (A) 25.0 mW cm^{-2} and (B) 50.0 mW cm^{-2} . The values are expressed as the means of three independent experiments; error bars indicate the standard deviation; DC—dark control; LC—light control. Lines combine experimental points.

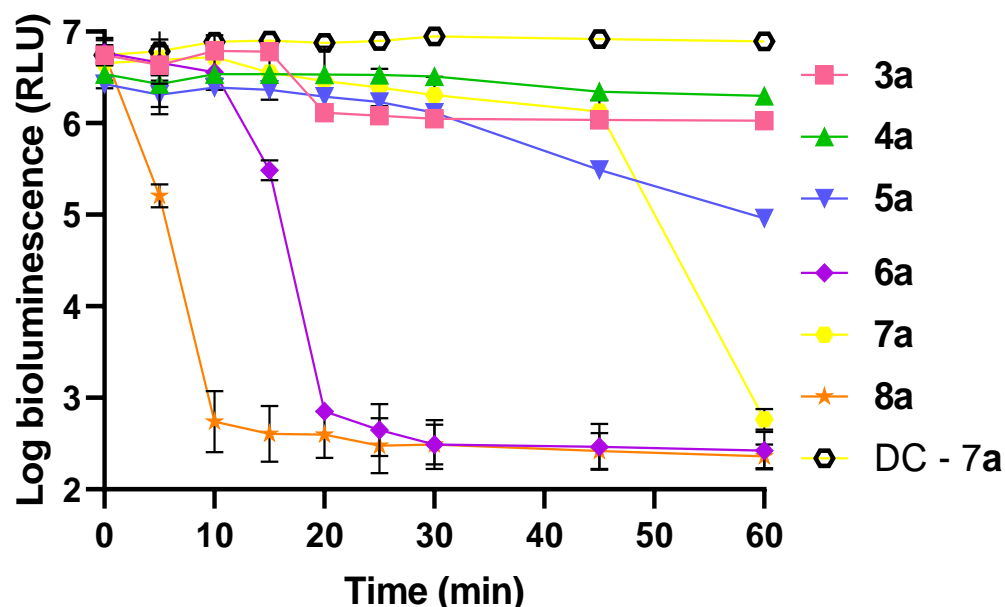


Figure 4. Comparison of photoinactivation of bioluminescent *E. coli* treated with methoxy pyridinium Pors 3a–5a and thiopyridinium Pors 6a–8a* at 5.0 μM at different irradiation times, under white light irradiation at 25.0 mW cm^{-2} . Values are expressed as means of three independent experiments; error bars indicate standard deviation. * The results for Pors 6a and 8a were described in the article [17].

For a better consistency in our study, it was related to the reduction in *E. coli* bioluminescence with the reduction expressed in $\log_{10} \text{CFU mL}^{-1}$ accomplished with the pour-plate methodology at times 0 and 60 min. The obtained results are presented as the average of the three assays in Figure 5. The obtained results for the Por-CD derivatives 3a–5a confirmed the results obtained through the bioluminescence monitoring of the PDI treatment. Only the conjugate 5a was able to generate a decrease of $\sim 1.5 \log$ (ANOVA, $p < 0.0001$) in the viability of *E. coli* after 60 min of light irradiation. Besides, at the same irradiance (25 mW cm^{-2}) and light exposure time (60 min), the Por-CD 7a caused a total photoinactivation of the *E. coli*, which corroborated the determined bioluminescence results, and is similar to the PDI results found in the literature for Por-CD 6a and 8a¹⁷). When the irradiance was increased to 50 mW cm^{-2} , Pors 3a–5a caused a decrease of $\sim 2 \log_{10}$ to $\sim 4 \log_{10}$ in the viability of *E. coli*, and Por 7a reached a complete bacteria inactivation. These results are in agreement with the RLU results found for photoinactivation bioluminescent

E. coli. All obtained results confirmed that the external positive charge and type of the cyclodextrin substituent of the Por-CD dyes considerably influences the PDI efficiency.

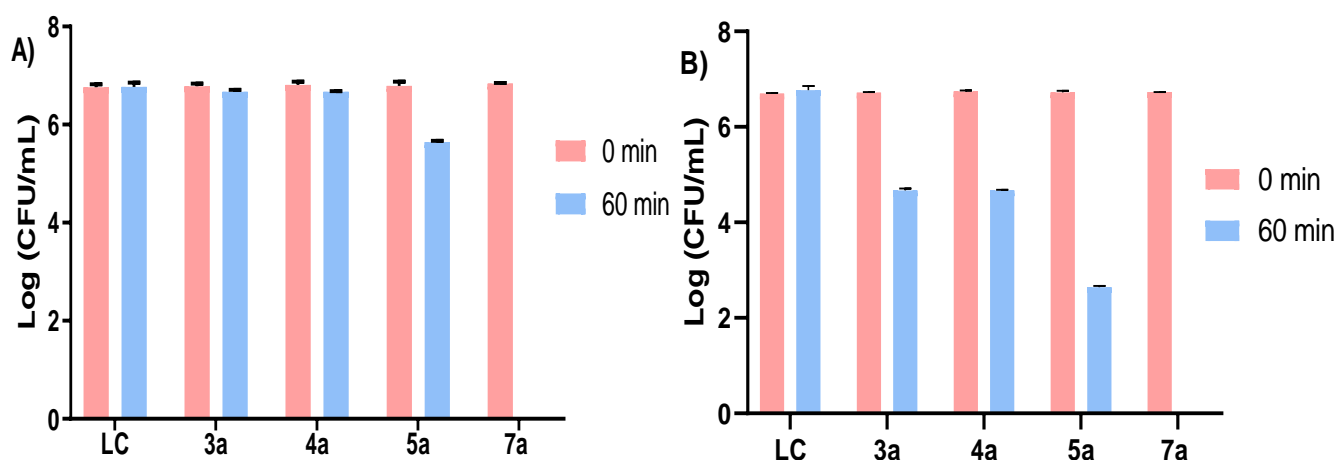


Figure 5. Photodynamic inactivation of bioluminescent *E. coli* treated with PSs 3a–5a and 7a at 5.0 μM after 60 min of white light irradiation at an irradiance of (A) 25 mW cm^{-2} and (B) 50 mW cm^{-2} . The values are expressed as the means of three independent experiments; error bars indicate the standard deviation.

It is well-known that the PS efficacy on the PDI treatments is correlated with different aspects, such as the microbial adsorption behavior, the ability of PS to generate singlet oxygen, the photostability profile, the solubility/aggregation compartment, or cell localization, among others [51]. Despite the fact that the ability to generate $^1\text{O}_2$ for all cationic Por derivatives, the γ -cyclodextrin derivatives (5a and 8a) were revealed to be better $^1\text{O}_2$ generators. This fact might justify the more efficient *E. coli* inactivation profile achieved for Por-CD conjugates 5a (3.5 \log_{10} reduction, 60 min, 50 mW cm^{-2}) and 8a (4.0 \log_{10} reduction, reaching the detection limit of the methodology, 15 min, 25 mW cm^{-2}), and it was more pronounced for 8a due to its highest $^1\text{O}_2$ generation, good water solubility, and the maximized electrostatic interactions between their more exposed peripheral positive charges and the Gram-negative bacterium. Moreover, different solubility profiles in the physiological medium of Por-CD derivatives can also justify the distinct PS inactivation behavior of *E. coli*. It is widely known that γ -cyclodextrin is more water-soluble than α -cyclodextrin [51,52], which clarifies the fact that Por derivatives 5a and 8a (γ -cyclodextrin derivatives) tend to have better PDI performances compared with the others Por-CD conjugates.

It is also important to highlight that the structural manner in which hydroxypyridine reacts with the Por structure (3a–5a) can also influence the photoinactivation efficiency. The substitution by the nitrogen, instead of the expected oxygen-bridge, as in a thio-bridge (6a–8a), probably makes the former less flexible. In addition, the position of the positive charge may also contribute to the aggregation behaviour in water once it is more protected from the aqueous environment. The position of the positive charge plays a key role in the physicochemical and biological features of the Por conjugates, evidencing that these features should be further addressed in the pursuit of optimized PS for antimicrobial photodynamic inactivation.

4. Conclusions

The new free-base Pors 3–5, 3a–5a, 7, and 7a were prepared and structurally characterized, and the photodynamic efficiency of the cationic Por-CD conjugates 3a–5a and 7a, as well as of the known Pors 6a and 8a, were evaluated against the bioluminescent strain of *E. coli*. The antimicrobial PDI assays within the series of 3a–5a (5.0 μM) showed that, only under white light at an irradiance of 50 mW cm^{-2} , a significant *E. coli* photoinactivation occurred. The Por 5a proved to be the best PS, causing a decrease of 3.5 and 4.0 \log_{10} of the bioluminescence signal after 30 and 60 min of light irradiation, respectively.

Analyzing the new inverted methoxypyridinium Pors **3a–5a** and the already-known thiopyridinium Pors **6a–8a**, at 5.0 μM at an irradiance of 25 mW cm^{-2} , a faster (in 30 min) and complete *E. coli* photoinactivation was confirmed, particularly for thiopyridinium Pors **6a** and **8a**. The obtained results show that the methoxypyridinium Por–CD conjugates (**3a–5a**) evidence less effectivity against the bacterial viability than the thiopyridinium Por–CD conjugates (**6a–8a**). According to the American Society of Microbiology, this is higher than the minimum required (reduction $> 3 \log \text{CFU mL}^{-1}$) for a new approach to be termed as antimicrobial. The Por **5a** (50 mW cm^{-2}) and Pors **6a–8a** (25 mW cm^{-2}) can be considered promising PS drugs for PDI.

Author Contributions: Conceptualization, L.M.O.L.; methodology, C.P.S.R.; validation, L.M.O.L., A.A., M.A.F.F. and C.P.S.R.; investigation, C.P.S.R.; resources, L.M.O.L., A.A. and M.A.F.F.; writing—original draft, C.P.S.R.; writing—review and editing, L.M.O.L., A.A., M.A.F.F. and C.P.S.R.; supervision, L.M.O.L. and A.A.; funding acquisition, L.M.O.L. and A.A. All authors have read and agreed to the published version of the manuscript.

Funding: This research was funded by FCT/MCTES, grant number UIDB/50006/2020, grant number UIDB/50017/2020 + UIDP/50017/2020, and grant number P2020-PTDC/QUI-QOR/31770/2017.

Institutional Review Board Statement: Not applicable.

Informed Consent Statement: Not applicable.

Data Availability Statement: Not applicable.

Acknowledgments: Thanks are due to the University of Aveiro and FCT/MCTES for the financial support to LAQV-REQUIMTE (UIDB/50006/2020) and CESAM (UIDB/50017/2020 + UIDP/50017/2020) research units, and to the FCT projects P2020-PTDC/QUI-QOR/31770/2017, through national funds (PIDDAC) and where applicable co-financed by the FEDER–Operational Thematic Program for Competitiveness and Internationalization–COMPETE 2020, within the PT2020 Partnership Agreement. Thanks, are also due to the Portuguese NMR and Mass Networks. C. Ribeiro thanks FCT for their PhD scholarships (UI/BD/152798/2022).

Conflicts of Interest: The authors declare no conflict of interest.

References

1. Lloyd-Price, J.; Abu-Ali, G.; Huttenhower, C. The healthy human microbiome. *Genome Med.* **2016**, *8*, 51. [[CrossRef](#)] [[PubMed](#)]
2. Percival, S.L.; Williams, D.W. Chapter Six—*Escherichia coli*. In *Microbiology of Waterborne Diseases*, 2nd ed.; Percival, S.L., Yates, M.V., Williams, D.W., Chalmers, R.M., Gray, N.F., Eds.; Academic Press: London, UK, 2014; pp. 89–117.
3. Wainwright, M.; Maisch, T.; Nonell, S.; Plaetzer, K.; Almeida, A.; Tegos, G.P.; Hamblin, M.R. Photoantimicrobials—Are we afraid of the light? *Lancet Infect. Dis.* **2017**, *17*, e49–e55. [[CrossRef](#)]
4. Calmeiro, J.M.D.; Dias, C.J.; Ramos, C.I.V.; Almeida, A.; Tome, J.P.C.; Faustino, M.A.F.; Lourenco, L.M.O. Comparative photodynamic inactivation of bioluminescent *E. coli* by pyridinium and inverted pyridinium chlorins. *Dye. Pigm.* **2020**, *173*, 107410. [[CrossRef](#)]
5. Lourenco, L.M.O.; Rocha, D.M.G.C.; Ramos, C.I.V.; Gomes, M.C.; Almeida, A.; Faustino, M.A.F.; Almeida Paz, F.A.; Neves, M.G.P.M.S.; Cunha, Â.; Tomé, J.P.C. Photoinactivation of planktonic and biofilm forms of *Escherichia coli* through the reaction of cationic zinc (II) phthalocyanines. *ChemPhotoChem* **2019**, *3*, 251–260. [[CrossRef](#)]
6. Calmeiro, J.M.D.; Gamas, S.R.D.; Gomes, A.T.P.C.; Faustino, M.A.F.; Neves, M.G.P.M.S.; Almeida, A.; Tome, J.P.C.; Lourenco, L.M.O. Versatile thiopyridyl/pyridinone porphyrins combined with potassium iodide and thiopyridinium/methoxypyridinium porphyrins on *E. coli* Photoinactivation. *Dye. Pigm.* **2020**, *181*, 108476. [[CrossRef](#)]
7. Heffron, J.; Bork, M.; Mayer, B.K.; Skwor, T. A Comparison of Porphyrin Photosensitizers in Photodynamic Inactivation of RNA and DNA Bacteriophages. *Viruses* **2021**, *13*, 530. [[CrossRef](#)]
8. Garcia, M.; David, B.; Sierra-Garcia, I.N.; Faustino, M.A.F.; Alves, A.; Esteves, A.C.; Cunha, A. Photodynamic inactivation of *Lasiodiplodia theobromae*: Lighting the way towards an environmentally friendly phytosanitary treatment. *Biol. Lett.* **2021**, *17*, 20200820. [[CrossRef](#)]
9. Souza, T.H.; Andrade, C.G.; Cabral, F.V.; Sarmiento-Neto, J.F.; Rebouças, J.S.; Santos, B.S.; Ribeiro, M.S.; Figueiredo, R.C.; Fontes, A. Efficient photodynamic inactivation of *Leishmania* parasites mediated by lipophilic water-soluble Zn (II) porphyrin ZnTnHex-2-PyP4+. *Biochim. Biophys. Acta (BBA)-Gen. Subj.* **2021**, *1865*, 129897. [[CrossRef](#)]
10. Foggiato, A.A.; Silva, D.F.; Castro, R.C.F.R. Effect of photodynamic therapy on surface decontamination in clinical orthodontic instruments. *Photodiagnosis Photodyn. Ther.* **2018**, *24*, 123–128. [[CrossRef](#)]

11. Bartolomeu, M.; Reis, S.; Fontes, M.; Neves, M.G.P.M.S.P.; Faustino, M.A.F.; Almeida, A. Photodynamic action against wastewater microorganisms and chemical pollutants: An effective approach with low environmental impact. *Water* **2017**, *9*, 630. [[CrossRef](#)]
12. Cossu, M.; Ledda, L.; Cossu, A. Emerging trends in the photodynamic inactivation (PDI) applied to the food decontamination. *Food Res. Int.* **2021**, *144*, 110358. [[CrossRef](#)] [[PubMed](#)]
13. Sawada, T.; Yasukawa, T.; Imaizumi, H.; Matsubara, H.; Kimura, K.; Terasaki, H.; Ishikawa, H.; Murakami, T.; Takeuchi, M.; Mitamura, Y. Ten-year changes in visual acuity at baseline and at 2 years after treatment in a Japanese population with age-related macular degeneration. *Graefes Arch. Clin. Exp. Ophthalmol.* **2021**, *259*, 1191–1198. [[CrossRef](#)] [[PubMed](#)]
14. Babu, B.; Sindelo, A.; Mack, J.; Nyokong, T. Thien-2-yl substituted chlorins as photosensitizers for photodynamic therapy and photodynamic antimicrobial chemotherapy. *Dye. Pigm.* **2021**, *185*, 108886. [[CrossRef](#)]
15. Silva, J.N.; Silva, A.M.G.; Tomé, J.P.C.; Ribeiro, A.O.; Domingues, M.R.M.; Cavaleiro, J.A.S.; Silva, A.M.S.; Neves, M.G.P.M.S.P.; Tomé, A.C.; Serra, O.A.; et al. Photophysical properties of a photocytotoxic fluorinated chlorin conjugated to four β -cyclodextrins. *Photochem. Photobiol. Sci.* **2008**, *7*, 834–843. [[CrossRef](#)]
16. Reynoso, E.; Ferreyra, D.D.; Durantini, E.N.; Spesia, M.B. Photodynamic inactivation to prevent and disrupt *Staphylococcus aureus* biofilm under different media conditions. *Photodermatol. Photoimmunol. Photomed.* **2019**, *35*, 322–331. [[CrossRef](#)]
17. Ribeiro, C.P.S.; Gamelas, S.R.D.; Faustino, M.A.F.; Gomes, A.T.P.C.; Tomé, J.P.C.; Almeida, A.; Lourenco, L.M.O. Unsymmetrical cationic porphyrin-cyclodextrin bioconjugates for photoinactivation of *Escherichia coli*. *Photodiagnosis Photodyn. Ther.* **2020**, *31*, 101788. [[CrossRef](#)]
18. Gonçalves, P.J.; Bezzerra, F.C.; Teles, A.V.; Menezes, L.B.; Alves, K.M.; Alonso, L.; Alonso, A.; Andrade, M.A.; Borissevitch, I.E.; Souza, G.R. Photoinactivation of *Salmonella enterica* (serovar Typhimurium) by tetra-cationic porphyrins containing peripheral [Ru (bpy) 2Cl]⁺ units. *J. Photochem. Photobiol. A Chem.* **2020**, *391*, 112375. [[CrossRef](#)]
19. Sagrillo, F.S.; Dias, C.; Gomes, A.T.P.C.; Faustino, M.A.F.; Almeida, A.; de Souza, A.G.; Costa, A.R.P.; Bochat, F.d.C.S.; de Souza, M.C.B.V.; Neves, M.G.P.M.S.; et al. Synthesis and photodynamic effects of new porphyrin/4-oxoquinoline derivatives in the inactivation of *S. aureus*. *Photochem. Photobiol. Sci.* **2019**, *18*, 1910–1922. [[CrossRef](#)]
20. Revuelta-Maza, M.Á.; Gonzalez-Jimenez, P.; Hally, C.; Agut, M.; Nonell, S.; de la Torre, G.; Torres, T. Fluorine-substituted tetracationic ABAB-phthalocyanines for efficient photodynamic inactivation of Gram-positive and Gram-negative bacteria. *Eur. J. Med. Chem.* **2020**, *187*, 111957. [[CrossRef](#)]
21. Ribeiro, C.P.S.; Lourenco, L.M.O. Overview of cationic phthalocyanines for effective photoinactivation of pathogenic microorganisms. *J. Photochem. Photobiol. C Photochem. Rev.* **2021**, *48*, 100422. [[CrossRef](#)]
22. Güzel, E.; Medina, D.-P.; Medel, M.; Kandaz, M.; Torres, T.; Morgade, M.S.R. A versatile, divergent route for the synthesis of ABAC tetraazaporphyrins, molecularly engineered, push-pull phthalocyanine-type dyes. *J. Mater. Chem. C* **2021**, *9*, 10802–10810. [[CrossRef](#)]
23. Gamelas, S.R.D.; Gomes, A.T.P.C.; Faustino, M.A.F.; Tomé, A.C.; Tomé, J.C.P.; Almeida, A.; Lourenco, L.M.O. Photoinactivation of *Escherichia coli* with Water-Soluble Ammonium-Substituted Phthalocyanines. *ACS Appl. Bio Mater.* **2020**, *3*, 4044–4051. [[CrossRef](#)] [[PubMed](#)]
24. Marciel, L.; Teles, L.; Moreira, B.; Pacheco, M.; Lourenco, L.M.O.; Neves, M.G.P.M.S.; Tomé, J.P.C.; Faustino, M.A.F.; Almeida, A. An effective and potentially safe blood disinfection protocol using tetrapyrrolic photosensitizers. *Future Med. Chem.* **2017**, *9*, 365–379. [[CrossRef](#)]
25. Ramos, C.I.V.; Almeida, S.P.; Lourenco, L.M.O.; Pereira, P.M.R.; Fernandes, R.; Faustino, M.A.F.; Tomé, J.P.C.; Carvalho, J.; Cruz, C.; Neves, M.G.P.M.S. Multicharged phthalocyanines as selective ligands for G-quadruplex DNA structures. *Molecules* **2019**, *24*, 733. [[CrossRef](#)]
26. Sridhar, K.; Inbaraj, B.S.; Chen, B.-H. Recent developments on production, purification and biological activity of marine peptides. *Food Res. Int.* **2021**, *147*, 110468. [[CrossRef](#)] [[PubMed](#)]
27. Alves, E.; Faustino, M.A.F.; Neves, M.G.P.M.S.; Cunha, Â.; Nadais, H.; Almeida, A. Potential applications of porphyrins in photodynamic inactivation beyond the medical scope. *J. Photochem. Photobiol. C: Photochem. Rev.* **2015**, *22*, 34–57. [[CrossRef](#)]
28. Pereira, M.A.; Faustino, M.A.F.; Tomé, J.P.C.; Neves, M.G.P.M.S.; Tome, A.C.; Cavaleiro, J.A.S.; Cunha, A.; Almeida, A. Influence of external bacterial structures on the efficiency of photodynamic inactivation by a cationic porphyrin. *Photochem. Photobiol. Sci.* **2014**, *13*, 680–690. [[CrossRef](#)]
29. Hamblin, M.R. Antimicrobial photodynamic inactivation: A bright new technique to kill resistant microbes. *Curr. Opin. Microbiol.* **2016**, *33*, 67–73. [[CrossRef](#)]
30. Simões, C.; Gomes, M.C.; Neves, M.G.P.M.S.; Cunha, Â.; Tomé, J.P.C.; Tomé, A.C.; Cavaleiro, J.A.S.; Almeida, A.; Faustino, M.A.F. Photodynamic inactivation of *Escherichia coli* with cationic meso-tetraarylporphyrins—The charge number and charge distribution effects. *Catal. Today* **2016**, *266*, 197–204. [[CrossRef](#)]
31. Abrahamse, H.; Hamblin, M.R. New photosensitizers for photodynamic therapy. *Biochem. J.* **2016**, *473*, 347–364. [[CrossRef](#)]
32. Mesquita, M.Q.; Dias, C.J.; Neves, M.G.P.M.S.; Almeida, A.; Faustino, M.A.F. Revisiting current photoactive materials for antimicrobial photodynamic therapy. *Molecules* **2018**, *23*, 2424. [[CrossRef](#)] [[PubMed](#)]
33. Santos, C.I.M.; Rodríguez-Pérez, L.; Gonçalves, G.; Pinto, S.N.; Melle-Franco, M.; Marques, P.A.A.P.; Faustino, M.A.F.; Herranz, M.Á.; Martin, N.; Neves, M.G.P.M.S.P.; et al. Novel hybrids based on graphene quantum dots covalently linked to glycol corroles for multiphoton bioimaging. *Carbon* **2020**, *166*, 164–174. [[CrossRef](#)]

34. Gomes, A.T.P.C.; Faustino, M.A.F.; Neves, M.G.P.M.S.P.; Ferreira, V.F.; Juarranz, A.; Cavaleiro, J.A.S.; Sanz-Rodríguez, F. Photodynamic effect of glycochlorin conjugates in human cancer epithelial cells. *RSC Adv.* **2015**, *5*, 33496–33502. [[CrossRef](#)]
35. Silva, S.; Pereira, P.M.R.; Silva, P.; Paz, F.A.A.; Faustino, M.A.F.; Cavaleiro, J.A.S.; Tomé, J.P.C. Porphyrin and phthalocyanine glycodendritic conjugates: Synthesis, photophysical and photochemical properties. *Chem. Commun.* **2012**, *48*, 3608–3610. [[CrossRef](#)] [[PubMed](#)]
36. Del Valle, E.M. Cyclodextrins and their uses: A review. *Process Biochem.* **2004**, *39*, 1033–1046. [[CrossRef](#)]
37. Carneiro, S.B.; Costa Duarte, F.Í.; Heimfarth, L.; Siqueira Quintans, J.d.S.; Quintans-Júnior, L.J.; Veiga Júnior, V.F.d.; Neves de Lima, Á.A. Cyclodextrin–drug inclusion complexes: In vivo and in vitro approaches. *Int. J. Mol. Sci.* **2019**, *20*, 642. [[CrossRef](#)]
38. Barata, J.F.; Zamarron, A.; Neves, M.G.P.M.S.P.; Faustino, M.A.F.; Tomé, A.C.; Cavaleiro, J.A.S.; Röder, B.; Juarranz, Á.; Sanz-Rodríguez, F. Photodynamic effects induced by meso-tris (pentafluorophenyl) corrole and its cyclodextrin conjugates on cytoskeletal components of HeLa cells. *Eur. J. Med. Chem.* **2015**, *92*, 135–144. [[CrossRef](#)]
39. Karginov, V.A. Cyclodextrin derivatives as anti-infectives. *Curr. Opin. Pharmacol.* **2013**, *13*, 717–725. [[CrossRef](#)]
40. Agnes, M.; Thanassoulas, A.; Stavropoulos, P.; Nounesis, G.; Miliotis, G.; Miriagou, V.; Athanasiou, E.; Benkovics, G.; Malanga, M.; Yannakopoulou, K. Designed positively charged cyclodextrin hosts with enhanced binding of penicillins as carriers for the delivery of antibiotics: The case of oxacillin. *Int. J. Pharm.* **2017**, *531*, 480–491. [[CrossRef](#)]
41. Castriciano, M.A.; Zagami, R.; Casaletto, M.P.; Martel, B.; Trapani, M.; Romeo, A.; Villari, V.; Sciortino, M.T.; Grasso, L.; Guglielmino, S. Poly (carboxylic acid)-cyclodextrin/anionic porphyrin finished fabrics as photosensitizer releasers for antimicrobial photodynamic therapy. *Biomacromolecules* **2017**, *18*, 1134–1144. [[CrossRef](#)]
42. Armarego, W.L.; Chai, C.L.L. *Purification of Laboratory Chemicals*; Armarego, W.L.F., Chai, C.L.L., Eds.; Elsevier: Amsterdam, The Netherlands, 2013.
43. Taniguchi, M.; Lindsey, J.S.; Bocian, D.F.; Holten, D. Comprehensive review of photophysical parameters (ϵ , Φ_f , τ_s) of tetraphenylporphyrin (H₂TPP) and zinc tetraphenylporphyrin (ZnTPP)—Critical benchmark molecules in photochemistry and photosynthesis. *J. Photochem. Photobiol. C Photochem. Rev.* **2021**, *46*, 100401. [[CrossRef](#)]
44. Ferreira, G.C.; Kadish, K.M.; Smith, K.M.; Guillard, R. *The Handbook of Porphyrin Science*; World Scientific: Singapore, 2013; Volume 27.
45. Mahajan, P.G.; Dige, N.C.; Vanjare, B.D.; Kim, C.-H.; Seo, S.-Y.; Lee, K.H. Design and Synthesis of New Porphyrin Analogues as Potent Photosensitizers for Photodynamic Therapy: Spectroscopic Approach. *J. Fluoresc.* **2020**, *30*, 397–406. [[CrossRef](#)] [[PubMed](#)]
46. Gomes, A.; Fernandes, E.; Lima, J.L.F.C. Fluorescence probes used for detection of reactive oxygen species. *J. Biochem. Biophys. Methods* **2005**, *65*, 45–80. [[CrossRef](#)] [[PubMed](#)]
47. Castro-Olivares, R.; Günther, G.; Zanicco, A.L.; Lemp, E. Linear free energy relationship analysis of solvent effect on singlet oxygen reactions with mono and disubstituted anthracene derivatives. *J. Photochem. Photobiol. A Chem.* **2009**, *207*, 160–166. [[CrossRef](#)]
48. Probst, A.; Mark, H.B., Jr.; Hansen, W.N. Simultaneous electrochemical and internal-reflection spectrometric measurements using gold-film electrodes. *J. Phys. Chem.* **1968**, *72*, 2576–2582. [[CrossRef](#)]
49. Vieira, C.; Gomes, A.T.P.C.; Mesquita, M.Q.; Moura, N.M.M.; Neves, M.G.P.M.S.P.; Faustino, M.A.F.; Almeida, A. An insight into the potentiation effect of potassium iodide on aPDT efficacy. *Front. Microbiol.* **2018**, *9*, 2665. [[CrossRef](#)] [[PubMed](#)]
50. Costa, D.C.; Pais, V.F.; Silva, A.M.; Cavaleiro, J.A.; Pischel, U.; Tome, J.P.C. Cationic porphyrins with inverted pyridinium groups and their fluorescence properties. *Tetrahedron Lett.* **2014**, *55*, 4156–4159. [[CrossRef](#)]
51. Zidovetzki, R.; Levitan, I. Use of cyclodextrins to manipulate plasma membrane cholesterol content: Evidence, misconceptions and control strategies. *Biochim. Biophys. Acta (BBA)-Biomembr.* **2007**, *1768*, 1311–1324. [[CrossRef](#)]
52. Hedges, A. Cyclodextrins: Properties and applications. In *Starch*; Elsevier: Amsterdam, The Netherlands, 2009; pp. 833–851.